JSMBE

http://publisher.uthm.edu.my/ojs/index.php/jsmbe

e-ISSN : 2821-3432

Journal of Structural Monitoring and Built Environment

Finite Element Analysis of Perforated Cold-Formed Steel Section: Effects of Shear Behaviour

Fatimah De'nan[1], Nor Salwani Hashim[1], Lee Kenth Zenth[1]

[1]School of Civil Engineering, Universiti Sains Malaysia,
14300 Nibong Tebal, Penang, MALAYSIA

*Corresponding Author

DOI: https://doi.org/10.30880/jsmbe.2021.01.01.003
Received 15 November 2021; Accepted 06 December 2021; Available online 31 December 2021

Abstract: This paper presents a numerical study on the shear behaviour of the steel framing system using a perforated section. The perforated steel section has a lower volume of steel, which causes the weight to decrease and lead to lower construction costs. However, perforation in steel will decrease the shear resistance of the steel framing system. The objective of this study was to investigate the shear behaviour of the perforated steel section comparing to the unperforated section in the steel framing system. Critical shear loading from a common steel framing system was obtained using Staad Pro software according to Eurocode Standard. Finite element analysis was performed and the structure capacity results were compared by using eigenvalue. Comparison were made between perforated sections and unperforated section in term of shear capacity and percentage of volume reduction. Perforation steel section with 8 diamond openings was selected with the percentage of shear buckling capacity difference from an unperforated section about 33.02% and 48.18% with circle openings. Shear buckling capacity reduced with the increasing number of web openings. Edge distance also affected the shear behaviour of plain channel section with web openings.

Keywords: Steel framing, perforated, shear behaviour, finite element analysis, eigenvalue

1. Introduction

Most of developing country, the population is increasing at a remarkable pace. To sustain a huge population, the construction of low-cost housing must be fast and affordable. Therefore, conventional low-cost housing construction which involve in-situ concrete, labor and formwork need to be improved. By using steel framing structure, precast and prefabricated formworks, housing construction has become faster, cheaper and cleaner compared to the concrete frame structure. Besides, steel structures can be erected easily and faster than other structures and can be used immediately compares to the concrete structure which required a curing period.

Perforated steel section is a steel member with holes used in air circulation, mechanical and electrical services installation. Nowadays, the perforated section is fabricated in a variety configuration and size which have a different impact on the structural performance. The openings on the web significantly reduce the shear area of the section (Tsavdaridis and D'Mello, 2009; Tsavdaridis et al., 2015). A lot of researches have been performed on steel I-section beams with a perforated section. Common perforated steel sections are castellated section (with hexagonal openings), and cellular section (with circular opening).

TriWP	triangular web profile

**Corresponding author: cefatimah@usm.my*

Perforated steel section is more useful for certain construction with determination of failure behaviour under the combined action of shear, moment and buckling. The presence of an opening in the web alters the stress distribution within the member and also influences its collapse behaviour. The shear transferred across sections with large openings is considered due to the loss of a web proportion. However, it is a better practice to locate the large opening remote from the high shear zones (Lawson, 1987). The provision of web openings in beams become a common engineering practice, to eliminate the probability to cut the holes subsequently in inappropriate locations which may contributed to structural failure. The introduction of web openings may cause decrement of the beam stiffness contributed to larger deflections than the conventional beams. This is due to the structure are subjected to high shear and heavy distortion causing high deformation of the section (Tsavdaridis and D'Mello, 2011; Tsavdaridis et al., 2013). Shear strength is decreased as the increment of web opening (Hamoodi and Gabar, 2013; Chan et al., 2013). However, shear behaviour of beams with perforation is more complicated because strengths are significantly reduced (Keerthan and Mahendran, 2013). The shear capacity of such beam is greatly influenced by the depth of the web opening (Darehshouri et al., 2013; Shan et al., 1997).

Despite all that, the perforated steel section can greatly reduce the cost as compared to the regular steel section without the perforated section and open-web steel joists (Zaarour and Redwood, 1996) due to the reduction in weight and volume. Besides that, cold-formed steel Lipped Channel Beams (LCB) with web openings are commonly used (Wanniarachchi et al., 2017). Moreover, using of cold-formed steel profile provide height strength besides sustainable, environmentalist, green building because it requires less material in structural systems (Tunca et al., 2018). Besides, the design of perforation improved the behaviour connections by enhancing ductility, rotational capacity and energy dissipation capacity (Tsavdaridis et al., 2014). However, the cost of a concrete framing system has increased almost comparable with the cost of a steel framing system. For an economical solution, the steel framing system can be enhanced by making openings at the web surface of the steel beam producing perforated steel section. The section will reduce the raw material required in the fabrication process as there are voids in the section. The proposed section is expected to have equal or slightly lesser shear capacity comparing to the section without openings. The available design equations are inadequate to determine the shear capacities of stainless steel beams with web openings (Fareed et al., 2019). Therefore, finite element analysis is performed to analyse the proposed section to study and investigate the engineering behaviours and performance of the proposed section with openings under shear loading.

2. Finite Element Analysis

This work was conducted using STAAD Pro (StaadPro, 2003) and LUSAS (Lusas, 2006) finite element software to develop perforated section models. The shear behaviour was assessed by obtaining the shear buckling capacity of the proposed section. The variables are the size of the opening, the shape of the opening, the spacing between opening, the position of opening and arrangement of opening. All proposed section models were compared to the control model which is a normal plain channel section. All models have a constant span of 1000 mm. The geometry of the proposed model can be referred to Bluescope Lysaght Plain Channel Steel Section LC15230 as shown in Fig. 1. The dimensions are; D, depth equalled to152 mm, B, breadth equalled to 51 mm and t, thickness equalled to 3 mm designs and R is channel radius.

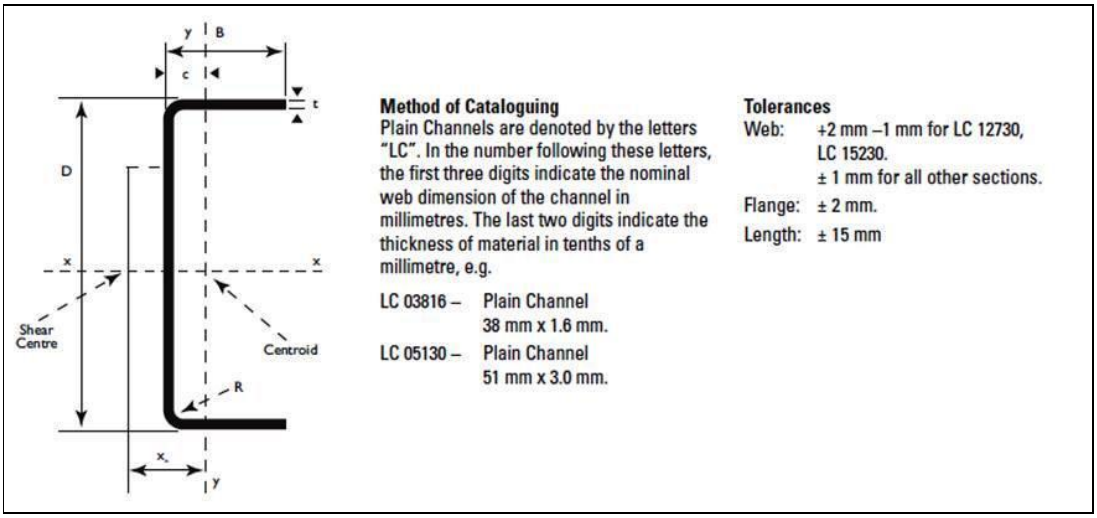

Fig. 1 - Dimension view of cold-formed plain channel steel section

Material assigned to the model is steel with the Young's Modulus of 200000 N/mm2 which is the average value for steel. The Poisson ratio used in this analysis is 0.3 for all the models. Eigenvalue shear buckling and deformation are considered. Circle and diamond opening shape with 0.4D is developed for analysis. 0.4D (where D is the depth of section) of opening diameter Ø are considered as follows:

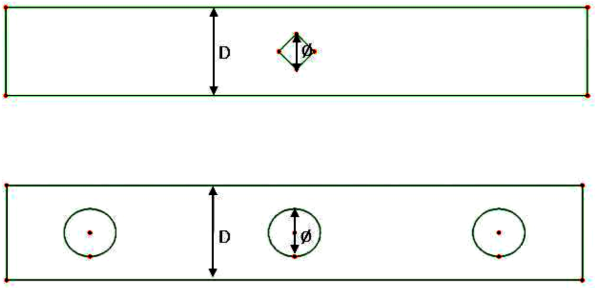

Fig. 2 - Dimension of web openings

Meshing describes the element type and discretisation on the model geometry. The type of meshing use in all the models is a thin shell. The order of interpolation of the meshing used is quadrilateral (QSL8). They are ideal for analysing flat and curved 3-dimensional shell structures where the transverse shear effects do not influence the solution.

Support and loading position as shown in Fig. 3 was adopted from Hasan, 2017; Eldib, 2009; Nie et al., 2013; Hamoodi and Gabar, 2013. The symbols of ABCD are presenting the location of the end nodes of the model. The support conditions for the model consist of pinned support at the left side end i.e. AB. It is constrained in x, y and z translation for pinned supported end. Meanwhile, along AC, CD, and BD, the supports are constrained in x and y translation. A concentrated load was exerted vertically (in the z-axis) to simulate a pure shear loading condition where the shear force due to applied concentrated load will be carried by the web. According to Hasan, 2017, the flanges are replaced with simple support boundary conditions for conservative consideration and models with or without flanges showed no changes in eigenvalue buckling and buckling modes.

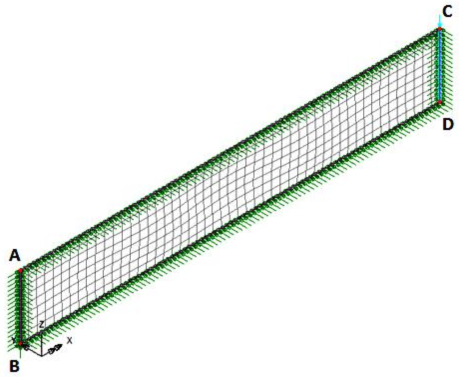

Fig. 3 - Finite element model

To identify the shear buckling capacity, eigenvalue analysis is used to analyse the shear buckling load of the plain channel section without opening. Shear buckling capacity is obtained by multiplying the actual magnitude of the applied loading with the load factor. Flow chart analyses are detailed as Fig. 4.

The convergence study begins by independently increasing the mesh density in each part of the model. Table 1 shows data of six models created with a different number of nodes and elements with respective results of maximum nodal displacement. To determine a suitable size of the element, a graph of maximum nodal displacements against the number of the element is plotted as shown in Fig. 5. From the graph, the convergence occurred when the number of elements is 850 with the size of elements of 20 mm. It is found that the increment in displacement becomes smaller from Model 1 to Model 6. As a result, the size of elements of 20 mm is used for analyses.

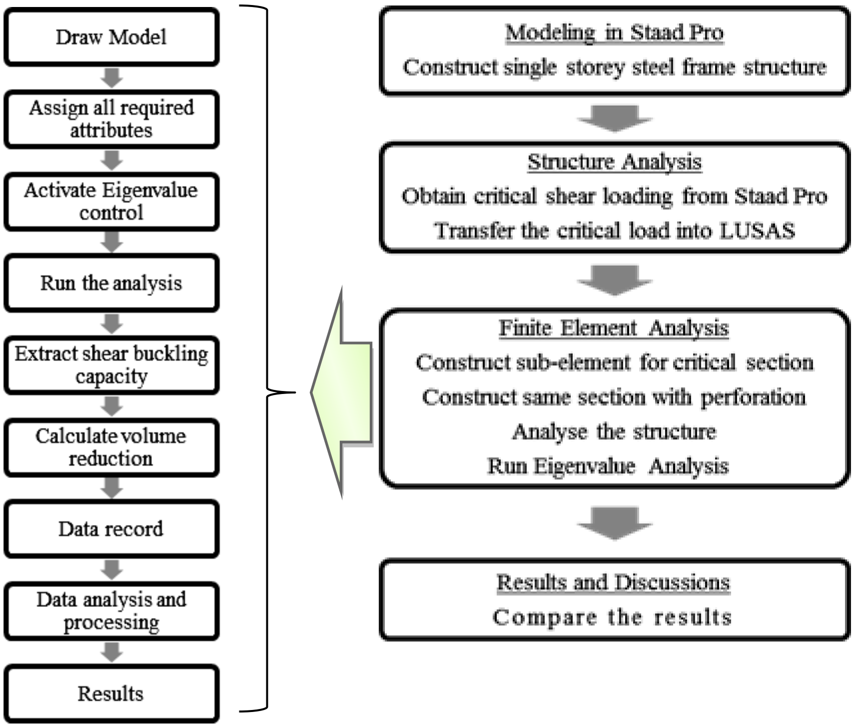

Fig. 4 - Finite element model

Table 1 - Maximum nodal displacements with different mesh sizes

Model	Number of elements	Number of nodes	Size of elements (mm)	Displacement (mm)
1	85	300	60	0.01594
2	120	413	50	0.01596
3	225	744	40	0.01606
4	396	1279	30	0.01608
5	850	2685	20	0.01609
6	3400	10469	10	0.01610

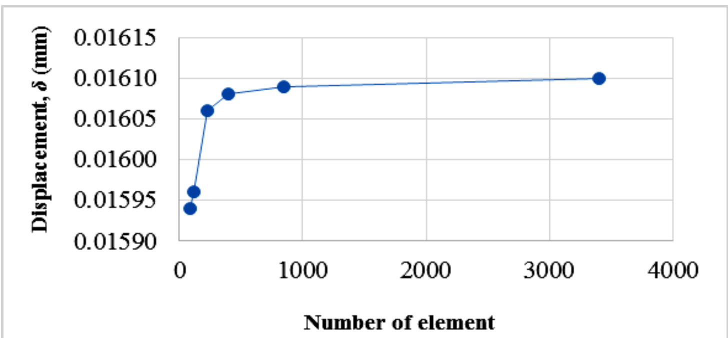

Fig. 5 - Graph of displacement against number of elements

3. Results

The model is Bluescope Lysaght Plain Channel 152 x 51 steel sections with different edge distance, opening spacing and opening shapes. 72 finite element models were produced and each model has the same 1000 mm of the span. The volume of each model is compared with the volume of plain channel section without web openings which are 744000 mm3. The reduction of the volume is calculated as the sample of the calculation shown in Table 2 and Table 3 below:

Table 2 - Dimension of perforated steel section with 0.4D circle shape

Radius of holes (mm)	No of openings	Net volume (mm^3)	Reduction of volume (%)
30.4	3	717869.99	3.51
30.4	4	709159.99	4.68
30.4	5	700449.99	5.85
30.4	6	691739.98	7.02
30.4	7	683029.98	8.19
30.4	8	674319.98	9.37
30.4	9	665609.97	10.54
30.4	10	656899.97	11.71
30.4	11	648189.97	12.88

Table 3 - Dimension of perforated steel section with 0.4D diamond shape

Diameter of holes (mm)	No of openings	Net volume (mm^3)	Reduction of volume (%)
60.8	3	727365.12	2.24
60.8	4	721820.16	2.98
60.8	5	716275.2	3.73
60.8	6	710730.24	4.47
60.8	7	705185.28	5.22
60.8	8	699640.32	5.96
60.8	9	694095.36	6.71
60.8	10	688550.4	7.45
60.8	11	683005.44	8.20

To identify the shear buckling capacity, eigenvalue analysis was used to analyse the shear buckling load of plain channel section without opening. Shear buckling capacity was obtained by multiplying the actual magnitude of the applied loading by the load factor. The load factor is equivalent to the eigenvalue calculated by eigenvalue buckling analysis. QSL8 element and the same material properties as plain channel section with various openings were applied in the model. The load and support conditions are the same for all models. Fig. 6 below shows the pattern of shear buckling of plain channel steel section. It shows from the shear buckling patterns that the typical shear buckling such as local buckling occurred in the webs.

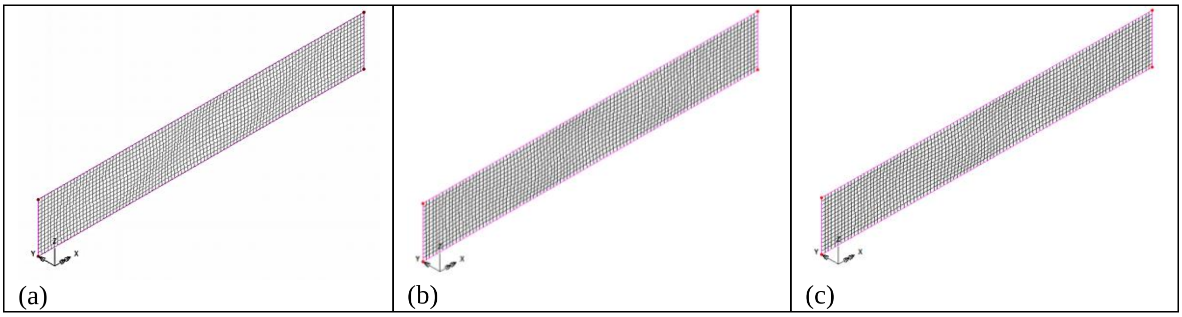

(a) (b) (c)

Fig. 6 - Pattern of shear buckling (a) eigenvalue 1 (b) eigenvalue 2 (c) eigenvalue 3

Fig. 7 shows the contours of the shear buckling mode from the eigenvalue analysis which occurred on the web. As the eigenvalue getting larger, the probability for the web shear buckling to occur becomes smaller. It can be observed that for eigenvalue 1, 2 and 3, local shear buckling had occurred with different orientation due to the pure shear condition set up.

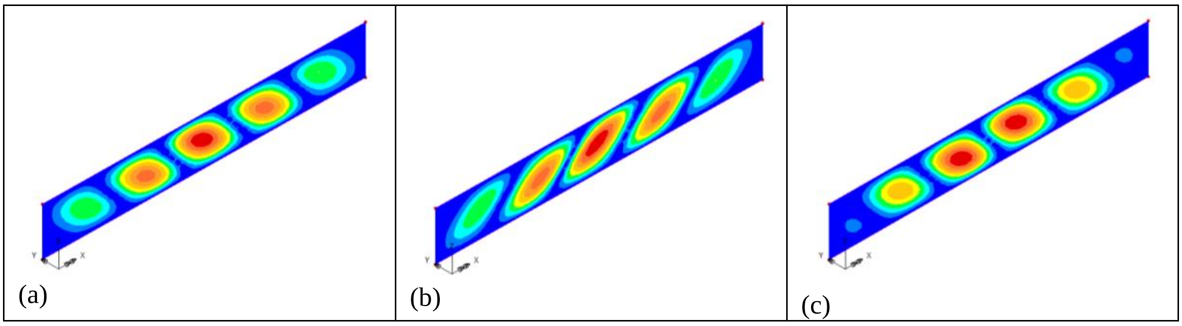

Fig. 7 - Local shear buckling (a) eigenvalue 1 (b) eigenvalue 2 (c) eigenvalue 3

The results of eigenvalue shear buckling analysis of plain channel section with different amounts of diamond openings and edge distance are presented below in Table 4. The shear buckling capacity comes from the shear buckling in the first mode shape. The shear buckling capacity of the plain channel without perforation is 10.17 kN. This value is then compared with shear buckling capacity of a plain channel with perforation and presented in Table 5. The percentage reduction of shear buckling capacity is then summarised.

Table 4 - Shear buckling capacity (kN) of plain channel section with diamond openings

No. of openings	Edge Distance (mm)				
	50	100	150	200	250
3	7.858	7.819	7.841	7.716	7.337
4	7.764	7.543	7.214	6.993	6.877
5	7.202	6.987	6.864	6.88	6.818
6	6.883	6.823	6.892	6.737	6.391
7	6.818	6.858	6.651	6.313	5.765
8	6.812	6.588	6.330	5.851	4.439
9	6.54	6.354	5.904	5.163	-
10	6.316	5.983	5.501	-	-
11	6.009	5.642	-	-	-

Table 5 - The percentage (%) difference of shear buckling capacity

No. of openings	Edge Distance (mm)				
	50	100	150	200	250
3	22.73	23.12	22.90	24.13	27.86
4	23.66	25.83	29.07	31.24	32.38
5	29.18	31.30	32.51	32.35	32.96
6	32.32	32.91	32.23	33.76	37.16
7	32.96	32.57	34.60	37.93	43.31
8	33.02	35.22	37.76	42.47	56.35
9	35.69	37.52	41.95	49.23	-
10	37.90	41.17	45.91	-	-
11	40.91	44.52	-	-	-

(-) Denote insufficient space for openings

Table 6 shows the results of eigenvalue shear buckling analysis of plain channel section with different amounts of circle openings and edge distance while Table 7 shows the percentage difference of shear buckling capacity between perforated sections with unperforated section. The shear buckling capacity from the plain channel with circle openings showed lower value. The volume reduction by circle openings is much larger compared to diamond openings as the volume of the web mainly contributes to shear resistance.

Table 6 - The shear buckling capacity (kN) of a plain channel with different no. of circle openings and edge distance

No. of openings	Edge Distance (mm)				
	50	100	150	200	250
3	6.823	6.77	6.795	6.696	6.355
4	6.723	6.521	6.235	5.955	5.717
5	6.202	5.955	5.758	5.624	5.471
6	5.833	5.705	5.627	5.415	4.908
7	5.634	5.545	5.318	4.879	4.252
8	5.494	5.274	4.916	4.363	1.704
9	5.27	4.889	4.484	3.315	-
10	4.917	4.53	3.904	-	-
11	4.526	4.008	-	-	-

(-) Denote insufficient space for openings

Table 7 - The percentage (%) difference of shear buckling capacity

No. of openings	Edge Distance (mm)				
	50	100	150	200	250
3	32.91	33.43	33.19	34.16	37.51
4	33.89	35.88	38.69	41.45	43.79
5	39.02	41.45	43.38	44.70	46.20
6	42.65	43.90	44.67	46.76	51.74
7	44.60	45.48	47.71	52.03	58.19
8	45.98	48.14	51.66	57.10	83.24
9	48.18	51.93	55.91	67.40	-
10	51.65	55.46	61.61	-	-
11	55.50	60.59	-	-	-

(-) Denote insufficient space for openings

Fig. 8 indicates that with an increasing number of openings, the shear buckling capacity also decreases simultaneously. By created 3 diamond openings on the web of the section, the shear buckling capacity decreased drastically by at least 22.7 % from its original value. This showed that the web mainly contributed to the shear strength of the plain channel section. The 11 number of openings and shear buckling capacity of 50 mm edge distance contributed higher shear buckling capacity comparing a maximum number of openings on other edge distance. Shear buckling capacity for lower edge distance with a different number of diamond openings provide better shear buckling capacity.

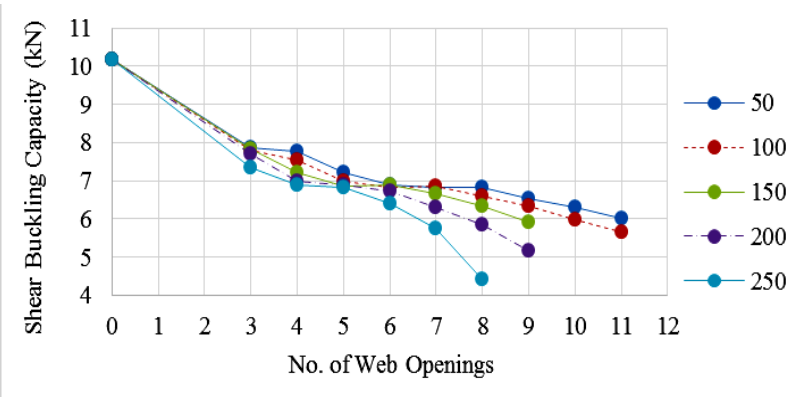

Fig. 8 - Shear buckling capacity of Lysaght plain channel against no. of diamond openings with different edge elements

Fig. 9 shows the trends of the percentage difference of shear buckling capacity of plain channel section with different number of diamond openings in different edge distance. The higher percentage difference, the lower shear buckling capacity of the section was observed. Although most trend lines show random fluctuation at lower edge distance, the trend still increases for increment in edge distance.

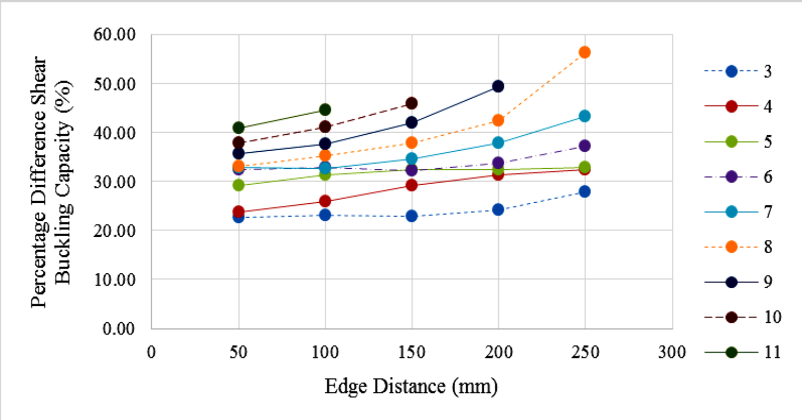

Fig. 9 - Trend of plain channel section with a number of diamond openings and different edge distance

From the results, the higher shear buckling capacity was noticed for the lower value of edge distance. However, for the 100 mm edge distance with 7 openings showed better shear capacity where different trends from other perforation section. For this analysis, a plain channel was modeled with 7 diamond openings because the section with 250 mm edge distance can only occupy up to maximum 7 openings. 100 mm edge distance with of 7 diamond openings was found a good optimum section. Despite all that, the differences between 50 mm and 100 mm edge distance for 7 diamond openings are still insignificant. Fig. 10 shows that shear buckling capacity of a plain channel with circle openings and different edge distance. For this type of opening, lower shear buckling capacity was observed with increment of edge distance.

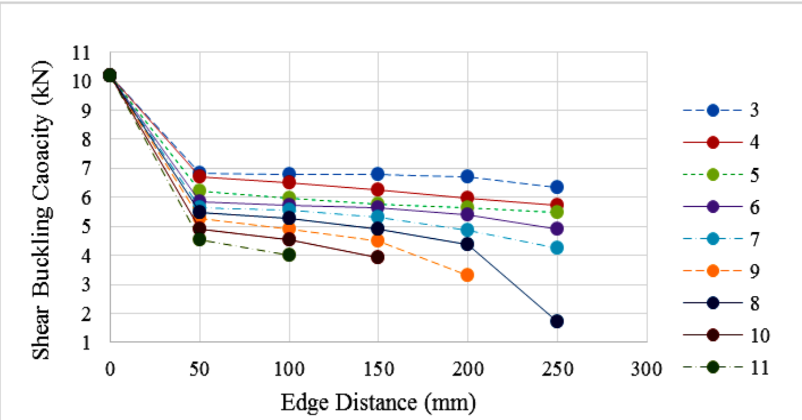

Fig. 10 - Shear buckling capacity against no. of circle openings with different edge distance

50 mm edge distance is chosen because this edge distance possesses higher shear buckling capacity comparing with others. To obtain the best volume reduction of steel material, the higher volume reduction and the lower shear buckling capacity must be considered. By subtracting these values, identification of optimum perforated plain channel section with better volume reduction while with higher shear capacity was observed. From Fig. 13, we can observe that perforated section with 8 openings gives a high percentage of volume reduction and acceptable shear buckling capacity. The 5 kN shear buckling capacity should be more than the critical shear force obtained from StaadPro. Fig. 11 shows a comparison of volume reduction percentage between diamond and circle openings. It was noticed that circle shape definitely reduced section volume more than diamond shape. The more percentage of volume reduction, the lighter section was found and reduce raw material production cost.

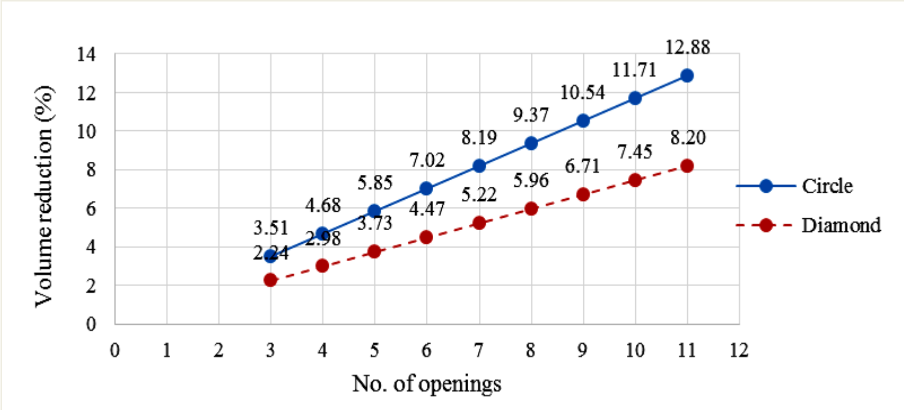

Fig. 11 - Percentage of volume reduction against no. of openings and different opening shapes with 50 mm edge distance

Fig. 12 shows shear buckling capacity against a number of openings and opening shapes with 50 mm edge distance. From the graph, diamond openings showed better shear buckling capacity compare to circle openings which agreed to Hassan, 2017 findings.

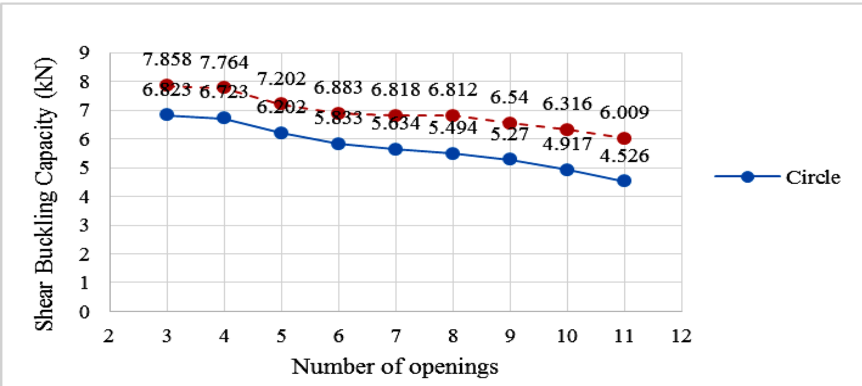

Fig. 12 - Shear buckling capacity against no. of openings and opening shape with 50 mm edge distance

Darehsouhri et al., 2013 stated that the ultimate shear buckling capacity was significantly influenced by the size of the opening; nearly 30% drop is observed when the depth of openings was increased to half the web depth of the girders. Besides, Hamoodi and Gabar, 2013 had found that the ultimate shear load of plate girder reduced about 51% with the presence of openings in the web section. Increasing perforation sizes will decrease the shear capacity of the section (Chan et al., 2013) as the presence of web openings can considerably reduce the shear strength of the section (Keerthan and Mahendran, 2013). However, the contribution of this analysis is to explore the reduction of shear in the web of cold-formed steel section. Besides, the lower edge distance introduced, the higher shear buckling capacity of the cold-formed plain channel section was concluded.

4. Conclusion

Based on finite element analysis results, the following conclusions were observed. The shear buckling capacity of Lysaght Plain Channel section without openings was 10.17kN. The critical shear loading obtained from the analysis of single-storey steel frame by Staad.Pro was 5kN. Therefore, Lysaght Plain Channel section was able to sustain the loads from single-storey steel.

Besides that, shear buckling capacity significantly reduced with existence of web openings. The result showed that section with 3 web openings, the shear buckling capacity reduced by 22.73% in diamond opening shape. A downtrend for shear buckling capacity results was observed with the increasing number of openings. As the edge distance increase, the shear buckling capacity of plain channel section with 3 diamond web openings dropped from 7.858 kN to 7.337 kN. Meanwhile, the percentage of volume reduction for plain channel section increased with an increasing number of web openings created. The percentage of volume reduction of plain channel section increased from 3.51% to 12.88% by creating 11 circle web openings. Thus, perforated plain channel section with 8 diamond web openings performed better in terms of shear behaviour. This section has 0.088% lesser than shear buckling capacity of the section with 7 web

openings but the volume of section reduced by 14.2% more. Perforated plain channel section with circle opening shape has lower volume of the section, thus the shear strength also reduces significantly.
The optimal section for Lysaght Plain Channel with web openings proposed was LC15230 with an eight 0.4D diamond-shaped web opening and 50mm edge distance with shear buckling capacity of 6.812kN and percentage of volume reduction of 5.96% if high shear strength required. However, for single storey affordable house steel framing system, the shear force required to sustain was 5kN. For raw material saving, Lysaght Plain Channel with 9 circle web opening and 50 mm edge distance was found an optimum section with the percentage of volume reduction of 10.54% and shear buckling capacity of 5.27 kN.

Acknowledgement

The authors are gratefully acknowledge with financial support by the Fundamental Research Grant Scheme (Account number: 203/PAWAM/6071239) during the course of this work.

References

"Bluescope Lysaght Plain Channel Section Catalogue" http://www.bluescopesteel.com.au/files/dmfile/coldformedsections1sectionpropertiesjan10.pdf, Jan 2010

Chan, R. W. K., Albermani, F. and Kitipornchai, S. (2013) Experimental study of perforated yielding shear panel device for passive energy dissipation. Journal of Constructional Steel Research, 91:14-25.

Darehshouri, S. F., Shanmugan, N. E. and Osman, S. A. (2013) "An analytical method for ultimate shear strength of composite plate girders with web openings." Engineering Structures, 56: 610-620.

Eldib, M. E. A.-H. (2009) "Shear buckling strength and design of curved corrugated steel webs for bridges." Journal of Constructional Steel Research, 65:2129-2139.

Fareed, I., Somadasa, W., Poologanathan, K., Gunalan, S., Corradi, M. and Sivapalan, S. (2019) "Finite Element Analyses of Cold-formed Stainless Steel Beam with WebOpenings in Shear." NORDIC STEEL 2019The 14th Nordic Steel Construction Conference,September 18–20, 2019, Copenhagen, Denmark, pp. 907-912

Hamoodi, M. J. and Gabar, M. S. A. (2013) "Behaviour of steel plate girders with web openings loaded in shear." Engineering and Technology Journal, 31:2982-2996.

Hasan, H. (2017) "The efficiency of I-beam steel section with perforated-corrugated web profile." Master Thesis. Universiti Sains Malaysia.

Keerthan, P. and Mahendran, M. (2013) "Experimental studies of the shear behaviour and strength of lipped channel beams with web openings." Thin-Walled Structures, 73:131-144.

Lawson, R. M. (1987) Design for openings in the webs of composite beam, CIRIA special publication 51, SCI publication 068.The Steel Construction Institute, Ascot.

LUSAS Modeller (2006) Version 14.0-3

Nie, J.-G., Zhu, L., Tao, M.-X. and Tang, L. (2013) "Shear strength of trapezoidal corrugated steel webs." Journal of Constructional Steel Research, 85:105-115.

Shan, M. Y., LaBoube, R. A., Langan, J. E. and Yu, W. W. (1997) "Cold-formed Steel Webs with Openings: Summary report," Thin-Walled Structures, 27:79 – 84.

STAAD Pro (2003) Structural Analysis and Design software, Bentley system

Tunca, O., Erdal, F., Sağsöz, A. E. and Çarbaş, S. (2018) "Structural features of cold-formed steel profiles." Challenge Journal of Structural Mechanics, 4(2):77 -81

Tsavdaridis, K. D. and D'Mello, C. (2009). "Finite element investigation of perforated steel beams with different web opening configurations," ICASS'09/IJSSD-Proceedings of Sixth International Conference on Advances in Steel Structures and Progress in Structural Stability and Dynamics, ICASS'09 Press, pp. 1-8

Tsavdaridis, K. D. and D'Mello, C. (2011) "Web buckling study of the behaviour and strength of perforated steel beams with different novel web openings shapes." Journal of Constructional Steel Research, 67:1605-1620.

Tsavdaridis, K. D., D'Mello, C. and Huo, B. Y. (2013) "Experimental and computational study of the vertical shear behaviour of partially encased perforated steel beams." Engineering Structures, 56:805-822.

Tsavdaridis, K. D., Faghih, F. and Nikitas, N. (2014) "Assessment of Perforated Steel Beam-to-Column Connections Subjected to Cyclic Loading." Journal of Earthquake Engineering, 18(8):1302-1325.

Tsavdaridis, K. D., Kingman, J. and Toropov, V. (2015). "Application of structural topology optimisation to perforated steel beams." Computers & Structures, vol. 158, pp.108-123.

Wanniarachchi, K. S., Mahendran, M. and Keerthan, P. (2017) "Shear behaviour and design of Lipped Channel Beams with non-circular web openings." Thin-Walled Structures, 119: 83-102

Zaarour, W. and Redwood, R. (1996) "Web Buckling in Thin Webbed Castellated Beams." J. Struct. Eng., 122(8):860-866.